

Crash Impact Modelling Of Security Bollard

Shih Kwang TAY, Bryan LIM and Shu Herng NG

Ministry of Home Affairs, Singapore

Abstract

This paper presents the findings from vehicular crash test of a security bollard system, as well as findings generated from numerical simulations using two different loading approaches in LS-Dyna[®]. The differences between the results from numerical simulations and test observations are explored by examining the velocity-time history profiles of the vehicle and the rotational response of the bollard.

The first approach involved a NCAC Chevrolet C2500 finite element pickup model impacting against the bollard model. Contact algorithm was defined to represent the contact of an impacting pickup with the bollard at the collision. In the second approach, the vehicle impact was instead represented by a force pulse generated from the actual crash testing. This approach greatly reduced the computational time required and the results showed good agreement with the vehicle model simulation applied in the earlier approach. These models can be useful tools for design work and provide alternative means to assess the performance of the security bollard system.

1. Introduction

There has been a shift in terrorist modus operandi (MO) from a parked vehicle-borne improvised explosive device (VBIED) to a penetrative ('rammed') attack [1]. These vehicle-borne threats are intended to deal maximum damage by gaining close proximity to the targeted asset. This close-in detonation, coupled with potentially large explosive payload, can deliver immense loading on the targeted asset, inducing structural failure and extensive human injury.

A perpetual challenge in developing protective solutions is that of cost-effectiveness i.e. achieving the required security level at minimal cost. Standoff distance is the most effective mitigation measure against blast-induced structural failures and human injuries. Having sufficient standoff distance significantly reduces resources in terms of design efforts and costs, which would otherwise be required to harden the building or vulnerable areas. Towards this end, vehicle security barriers (VSB) provide the perimeter protection to a defined secured area, thereby enforcing the requisite standoff distances and keeping the threats away from the intended targets. Guidance on the selection, installation and use of vehicle security barriers are well covered in literature such as British Standards Institution (BSI) PAS69:2006 [2] and Unified Facilities Criteria UFC 4-022-02 [3].

Finite element modelling has been widely used for crash impact analysis such as crashworthiness study and design of roadside barriers. While vehicle crash tests are necessary for the validation of VSB designs, they are very resource intensive to plan and conduct. In this regard, numerical simulations are able to reduce the number of crash tests needed to analyze the robustness of

design. Although numerical simulations are powerful design tools to evaluate and predict product performance, they are also strongly discouraged by BSI PAS68:2010 [4] and ASTM F2656 – 07 [5] to field a product based on results from computer simulations alone. The implemented VSB would still require a full-scale vehicle impact test to be undertaken.

Crash impact reconstruction based on crash test data to generate various collision pulse model is not a new methodology. Analytical techniques that aim to represent real-world collision scenarios have been developed and commonly used in crashworthiness study. Detailed discussions on impact pulse modelling can be found in studies for vehicle safety research [6] and also in vulnerability assessments of concrete columns under low elevation vehicular impacts [7].

The study presented in this paper forms part of Singapore's Ministry of Home Affairs (MHA) technological development work on hostile vehicle mitigation and means to counter possible attacks by vehicle-borne threats. Two bollard designs were developed as part of this development effort. For validation purposes, full-scale vehicle crash tests were conducted on two different bollard systems, termed as Shallow Foundation Bollard (SFB-1) and Surface Mounted Bollard (SMB-1), respectively.

2. Test Description

Unlike roadside safety barriers, which are designed to enhance roadside safety by redirecting shallow angle impact of accidental collisions, VSB are designed against high angle and high energy penetrative hostile vehicle attacks. There are two internationally recognized crash testing standards to verify that a VSB can perform as intended. The bollard designs in this study were impacted in accordance to UK BSI PAS68:2010 impact test method. This test standard nominates five types of vehicles and seven test speeds as the impact conditions and assigns the corresponding classification ratings to the tested VSB. For the purpose of this paper, we are focusing on one of the vehicular mass and speed combination.



Figure 1: N1G - Toyota Hilux 4x4 single cab pick-up

The test vehicle chosen for the comparative study was an N1G, Toyota Hilux 4x4 pick-up. The vehicle was propelled via a winch cable to deliver a 90 degree impact at 48km/h on the middle bollard of a triple bollard assembly (See Figure 2). Accelerometers were mounted on the test vehicle to record the vehicle deceleration profile during the vehicle impact. High-speed cameras

were also deployed in accordance with the requirements of the impact test standard, to capture the impact sequence, vehicle and bollard assembly response.



Figure 2: Pre and post impact images: SFB-1 (left) & SMB-1 (right)

3. Overview of Bollard Model in LS-DYNA

The triple bollard assembly including the concrete foundation was modelled in LS-PrePost[®]. Displacement restraints were imposed on the boundary nodes of the concrete foundation, assuming that there is no movement of the foundation. The entire bollard assembly was created using shell elements. All the shell elements and vehicle model were modelled with approximately equivalent mesh sizes.

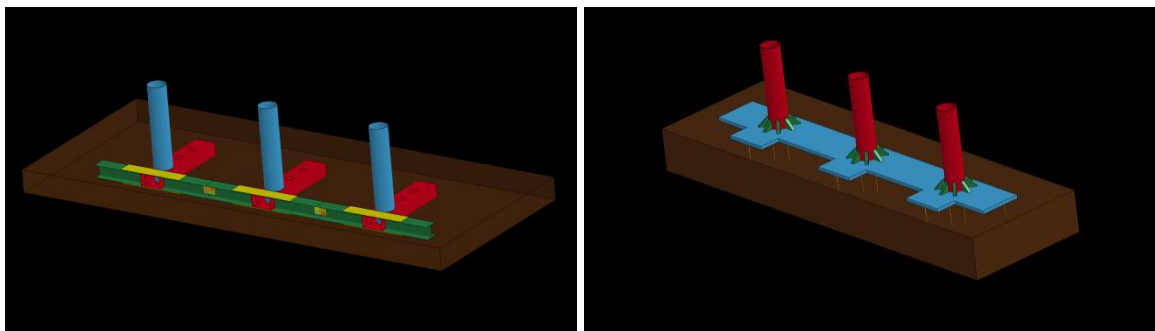


Figure 3: Model of SFB-1 (left) and SMB-1 (right) in LS-DYNA

Figure 3 shows an overview of the bollard models created using LS-Pre-Post. The steel element in both bollard models was represented by fully integrated shell elements. Hourglass control IHQ = 8 was also defined to activate the full projection warping stiffness. The steel material was defined using *MAT_24 (*MAT_PIECEWISE_LINEAR_PLASTICITY) with viscoplastic formulation VP = 1.0. A series of true stress-strain curves based on the Dynamic Increase Factor (DIF) for both yield and ultimate strength [8] were derived from a set of base engineering stress-strain curve. The same technique was similarly adopted by Tan S.H. et al [9] to define the steel material for close-in blast effects where strain rate effects are even more significant.

A mesh sensitivity exercise was conducted on 3 mesh configurations of the bollard model, i.e. 20mm, 10mm and 5mm. This is to investigate the numerical error in the model due to discretization so as to verify the calculations based on the Grid Convergence Index (GCI) [10]. The GCI calculations essentially estimate a zero-mesh-size converged solution using extrapolation and thus provide an estimate of the error that exists in the computed responses due to the selected mesh discretization. For this study, a GCI of 7.04% was obtained. The mesh refinement study was limited to the bollard assembly model, while the finite element vehicle model maintained the same mesh size.

3.1 SFB-1 Model

The concrete foundation of the bollard was represented by 8-nodes constant stress solid elements. *Mat_72R3 (*MAT_CONCRETE_DAMAGE_REL3) and viscous form hourglass control type 3 was used for the concrete material. Unconfined compressive cylinder strength of 25MPa (which correlated approximately with 30MPa cube strength [11]) was defined in the keyword card to auto-generate the concrete model parameters. In order to represent the bollard assembly within the subsurface of the concrete foundation without extensive modelling work, *CONSTRAINED_LAGRANGE_IN_SOLID with CTYPE = 2 was used in the same manner as coupling steel reinforcement to concrete elements [12].

The individual bollards were connected via the I-beams which were bolted together using two connecting plates. The bolt connection between the two plates were modeled using *CONSTRAINED_NODAL_RIGID_BODY by defining a set of nodes in the area as a rigid body.

The steel parts in the bollard assembly were primarily connected using fillet welds and these welds were represented in the numerical model by merging the nodes that coincided at the interfaces of the parts in question. Two contact keywords were used to define the various types of interaction within the bollard assembly model [13]. For some of the welding interfaces where there were geometrical complexity, the contact keyword *CONTACT_TIED_NODES_TO_SURFACE was used to join the steel parts. *CONTACT_AUTOMATIC_SINGLE_SURFACE was used to simulate the contact between the connecting plates and the I-beams.

3.2 SMB-1 Model

As shown in Figure 4, the anchoring system was represented by beam elements ELFORM = 1 Hughes-Liu with cross section integration and steel material represented by *MAT_24

(*MAT_PIECEWISE_LINEAR_PLASTICITY) with viscoplastic formulation $VP = 1.0$ similar to the bollard steel. The anchors share the same node as the assembly base plate at the top and the remaining length embedded in the concrete foundation using *CONSTRAINED_LAGRANGE_IN_SOLID with $CTYPE = 2$. It was assumed that the resin of the adhesive anchor was sufficient to prevent bolt pull-out thus the adhesive properties were not explicitly modeled in the simulation.

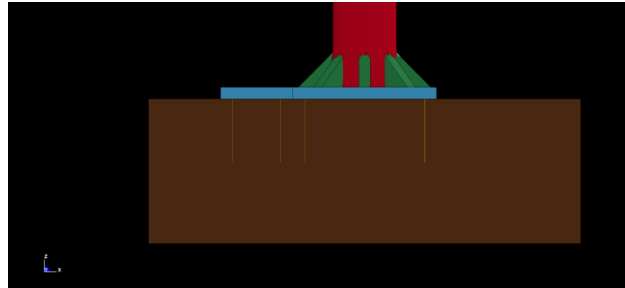


Figure 4: Model of SMB-1 anchoring bolts

Similar to SFB-1 model, the concrete foundation of the bollard was represented by 8-nodes constant stress solid elements. *MAT_159 (*MAT_CSCM_CONCRETE) was used to represent the concrete foundation that constrains the bolt. Unconfined compressive cylinder strength of 25MPa (which correlated approximately with 30MPa cube strength [11]) was defined to auto-generate the concrete model parameters.

The welded interfaces of the steel parts were modeled by merging coincident nodes. At locations where the fins interfaced with the base plate, the nodes did not coincide as a result of the different mesh configurations. *CONTACT_TIED_SHELL_EDGE_TO_SURFACE was thus used to join the fins to the base plate and the contact keyword allows the transfer of bending moment through the shell elements.

4. Vehicle Model Impact

The vehicle model applied in the simulation was an open source finite element model, Chevrolet C2500 pickup truck from National Crash Analysis Center (NCAC) [14]. Although the vehicle model is not validated to such high energy collision mode against a security barrier system, the study was carried out to assess the suitability of this FE vehicle model to provide a reasonable gauge of bollard performance against crash impact. As the weight of the vehicle model was lower than the actual crash test vehicle used, an additional cargo was created and loaded onto the vehicle cargo bed of the vehicle model. The cargo was connected to the vehicle model by shared nodes and the total mass was verified through the d3hsp file.

*CONTACT_AUTOMATIC_SURFACE_TO_SURFACE was defined between the FE vehicle model and the bollard assembly. A series of parametric tests were conducted to investigate the coefficient of friction parameter. It was found that this parameter did not significantly affect the average contact forces and rotational response of the bollard. Consequently, the coefficient of friction was set to 0.1 which was a reasonable value for metal contact [15].

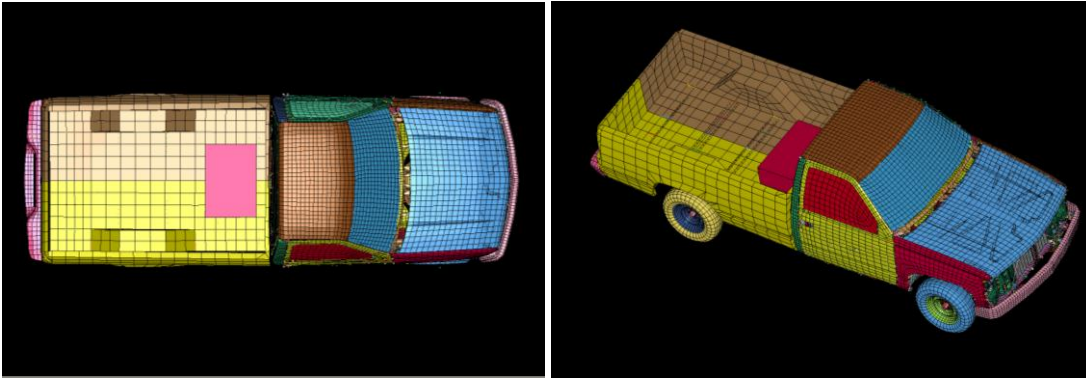


Figure 5: NCAC finite element model of pickup truck

5. Crash Pulse Modelling

Vehicle crash pulse was modeled based on the crash test data fitted with closed form functions. Three crash pulse formulations, namely haversine (\sin^2), sine and triangular were explored and discussed in this study. The crash pulse is a function of delta-V and duration of the crash (T_c). These two parameters were identified from the filtered acceleration and velocity history curves. For this study, the concept reported by Linder, A. et al [16] of deriving the delta-V and duration of crash was adopted, where T_c was defined as the time when the acceleration changed from positive to negative after 90% of delta-V had occurred.

As highlighted by Michael, S. V. [6], there are numerous factors that affect the characteristics of the pulse, such as vehicle shape, mass and barrier type. Given that only one impact mode was conducted using same vehicle and barrier type, more in-depth studies need to be conducted to investigate the correlation between the crash pulse model and the parameters.

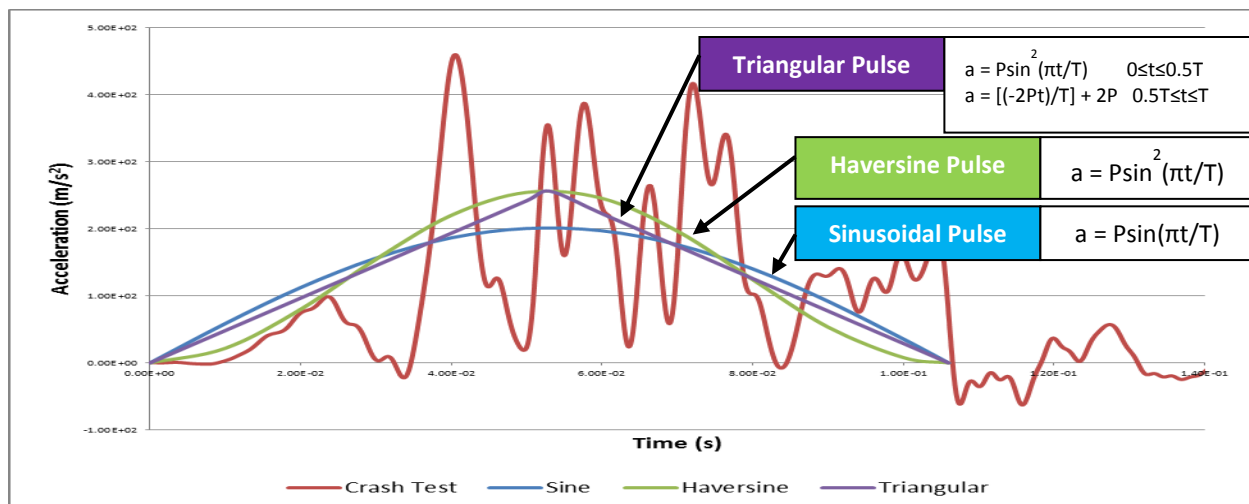


Figure 6: Acceleration time history of the derived crash pulse and actual test

Figure 6 shows the three crash pulse models plotted with the actual test acceleration time history. The acceleration curves were then integrated with respect to time and the obtained velocity curves were plotted with the actual velocity time history shown in Figure 7.

The load pulse for the three models was computed and plotted into a load-time history. A total of 20 segments were defined along the height of impact using *SET_SEGMENT. The height of impact was 640mm above ground which was akin to the actual crash testing vehicle impact height. The area of contact between the vehicle and bollard interaction was not investigated. A uniform normal pressure distribution was assumed and applied to the group of segments instead of a single point load to avoid stress singularity.

6. Results from the Crash Impact Analysis

Figure 7 shows the velocity-time history acquired from the crash test results as well as the results generated from the numerical simulation. This check was for the purpose of verifying a reasonable match between the outputs from three crash pulse models, the finite element vehicle model and the actual crash test data.

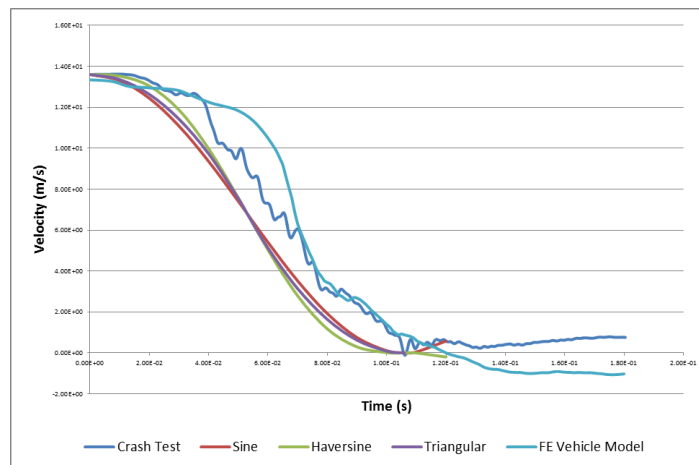


Figure 7: Velocity time history of the derived crash pulse and actual test

Figure 8 shows the collision simulation of the finite element pickup model impacting the SFB-1 and SMB-1 bollard systems. The hourglass energy for both simulation runs was approximately 7% of the internal energy. The vehicle was stopped by the bollard in both simulation runs. No penetration was recorded from the base of the ‘A’ pillar of the pickup to the rear face of bollard.

In order to quantify the performance of the bollard system, the peak rotational response of the bollard was recorded for comparison. It was observed that the bollard deflection obtained from the finite element vehicle model simulation was higher as compared to the actual deflection measured in the crash test. Notwithstanding the inherent difference in vehicle model used in numerical simulation (Chevrolet pickup) versus actual crash test (Toyota Hilux) to replicate similar collisions, the findings provided useful observations to assist in analyzing the bollards’ performance.

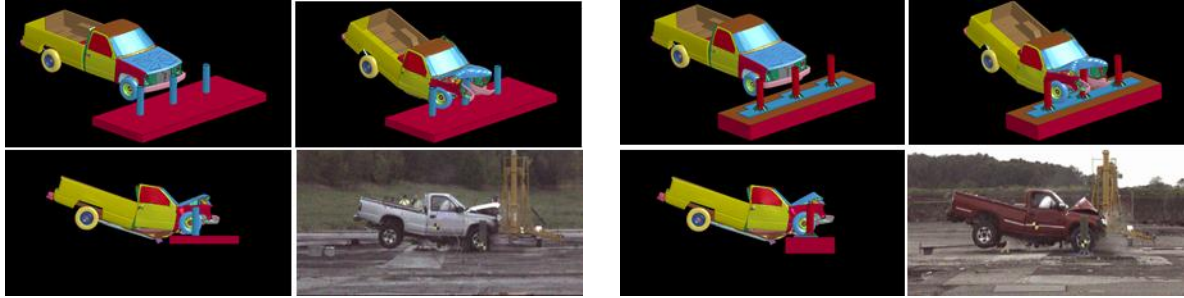


Figure 8: Simulation of vehicle model impacting SFB-1 model (left) and SMB-1 model (right)

For the numerical simulation runs conducted using the three crash pulse, these models were applied on the SMB-1 model and Figure 9 shows the rotational responses generated with the crash pulse models as compared to that involving the finite element vehicle model. The crash pulse models were found to yield results that correlated well with those from the crash test. The Sine pulse in particular resulted in a 0.24° rotation (final state) which agreed very well to the actual test that yielded 0.3° rotation.



Figure 9: Bollard rotational response

The application of crash pulse in place of the vehicle model greatly reduced the computational time required. Simulation runs using the vehicle model took approximately 6.5 times as much CPU time as those that applied the crash pulse approach. However, the study noted that the crash pulse approach had some inherent limitations compared to the finite element vehicle model approach. For example, the former precluded analysis of vehicle penetration and whether the vehicle will be launched over the barrier upon impact.

7. Conclusions

In this paper, two different loading approaches were demonstrated to simulate crash impact against a security bollard system. This study suggested that in the absence of a correlated vehicle model to simulate a particular crash impact scenario, crash pulse modelling offers an alternative approach in assessing impact performance of the VSB. Detailed investigation work on impact reconstruction using crash pulse for application on various modes of collision will be part of future study in building more accurate models.

8. References

- [1] Paul Forman et al. "Vehicle-borne threats and the principles of hostile vehicle mitigation", Blast effects on buildings, 2nd Edition, 2009
- [2] British Standards Institution. Guidance for the selection, installation and use of vehicle security barriers. Publicly Available Specification PAS 69: 2006. BSI, London, 2006.
- [3] UFC 4-022-02 (8 June 2009). Unified Facilities Criteria (UFC): Selection and Application of Vehicle Barriers
- [4] British Standards Institution. Impact test specifications for vehicle security barriers. Publicly Available Specification PAS 68: 2010. BSI, London, 2010.
- [5] ASTM F2656-07. Standard Test Method for Vehicle Crash Testing of Perimeter Barriers
- [6] Michael, S. V. et al. "Crash Pulse Modeling for Vehicle Safety Research", Proceedings 18th International Technical Conference on Enhanced Safety of Vehicles
- [7] Thilakarathna, H. M. I. et al. "Numerical simulation of axially loaded concrete columns under transverse impact and vulnerability assessment", International Journal of Impact Engineering 37 (2010) 1100-1112
- [8] Malvar, L. J., "Review of Static and Dynamic Properties of Steel Reinforcing Bars", ACI Materials Journal, Volume 95, No. 5, September-October 1998, Page 609 - 616
- [9] Tan, S.H. et al. "Retrofitting of Reinforced Concrete Beam-Column via Steel Jackets against Close-in Detonation", 12th International LS-Dyna Users Conference, 2012
- [10] ASME V&V 20-2009. Standard for Verification and Validation in Computational Fluid Dynamics and Heat Transfer
- [11] BS EN 1992-1-1:2004. Eurocode 2: Design of Concrete Structures – Part 1-1: General rules and rules for buildings
- [12] LS-DYNA Support, <http://www.dynasupport.com>
- [13] Contact Modeling in LS-DYNA by Suri Bala
- [14] NCAC. National Crash Analysis Centre (<http://www.ncac.gwu.edu/about.html>)
- [15] Paul Du Bois. Modeling & Simulation with LS-DYNA
- [16] Linder, A. et al. "Change of Velocity and Pulse Characteristics in Rear Impacts: Real World and Vehicle Tests Data", Proceedings 17th International Technical Conference on Enhanced Safety of Vehicles, Amsterdam, 2001